Effect of Ligand Backbone on the Selectivity and Stability of Rhodium Hydroformylation Catalysts Derived from Phospholane-Phosphites

José A. Fuentes,† Mesfin E. Janka,‡ Jody Rodgers,‡ Kevin J. Fontenot,‡ Michael Bühl,† Alexandra M. Z. Slawin† and Matthew L. Clarke†*

†EaStCHEM School of Chemistry, University of St Andrews, Purdie Building, North Haugh, St Andrews, KY16 9ST, United Kingdom). ‡Eastman Chemical Company, 200 South Wilcox Drive, Kingsport, Tennessee, 37660, USA

ABSTRACT: A study on how ligand backbone structure has an impact in selectivity, rate and catalyst stability of hydroformylation catalysts was prompted by some longer-term stability issues being discovered for a phospholane-phosphite with a [-CH_2O-] backbone. A series of phospholane-phosphite ligands were synthesized. Catalysts made *in situ* from these ligands and [Rh(acac)$(CO)_2$] were found to give *iso*-butanal selectivities up to 75% at temperatures between 75 and 105 °C: the latter being a benchmark for *iso*-selectivity in reactions conducted at industrially meaningful temperatures. A racemic rhodium complex of a bidentate phospholane-phosphite from a *tropos*-biphenol with an extended backbone showed unusually high stability at high temperatures, combined with even better *iso*-selectivity in propene hydroformylation relative to the original complex. A related ligand with an electron-withdrawing group maintained the unusually high stability and improved activity. Characterization of the pre-catalysts of type [$RhH(CO)_2$(L)] was accomplished using *in situ* HPIR spectroscopy and backed up by density functional theory calculations (B3PW91-D3 level), and by NMR studies; the latter showed the variation of the backbone also had a pronounced impact on pre-catalyst structure. A key finding is that it is now possible to prepare phospholane-phosphite ligands that deliver high *iso*-butanal selectivity, and that show no signs of degradation after several days even above typical reaction temperatures. In one stability test, several kilograms of aldehydes were produced with TOF and selectivity being consistent over several days.

INTRODUCTION

Hydroformylations of short chain alkenes such as propene are very important industrial processes.[1] Whilst *n*-butanal and products derived from it are produced in the largest quantities, *iso*-butanal derived products are also a very significant market.[2] Until recently, the innate preference for almost all known ligand-modified Rh catalysts to favour the linear aldehyde, at least to some extent,[3] meant that the best *iso*-butanal selectivities from hydroformylation of propene were quite close to 50/50. Moreover, the leading catalysts for producing more *iso*-butanal also tended to operate at low temperatures that lead to slow rates.[4] For the last decade we have been engaged in a project seeking to increase the proportion of *iso*-butanal that can be made in the hydroformylation of propene. We recently reported *iso*-butanal selectivity up to 82% at near-ambient temperature and, more significantly, *iso*-selectivity of around 60-65% at temperatures in the range used for industrial hydroformylation processes (75-90 °C) where faster rates were observed.[5] Our lead ligand from this part of the project was **2**, chosen over equally good enantiomerically pure catalyst (R_{ax},*R*,*R*)-**1**, Bobphos (Figure 1) since it is cheaper to produce.

During longer multi-day testing of the catalyst, we found that catalysts that display perfectly adequate stability for shorter preparative experiments started to degrade over time when operated at 80 °C or above, making them unsuitable for an industrial process that operates for extended time periods. This has led us to study how ligand structure impacts upon selectivity, rate and catalyst stability.

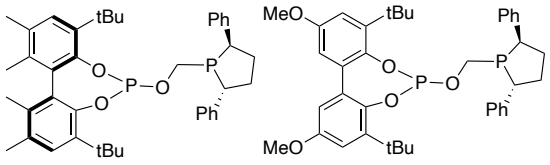

(*R*ax,*R*,*R*)-**1** *tropos*,*rac*-**2**

Figure 1. Lead ligands in the hydroformylation of propene

Here we show that the nature of the backbone connecting the two phosphorous atoms in these bidentate ligands has a pronounced effect on these aspects of performance and describe a highly stable *iso*-selective hydroformylation catalyst.

RESULTS AND DISCUSSION

In addition to the inherent susceptibility to hydrolysis of phosphites,[6] we speculated that from a stability perspective the P, O acetal structure of ligands **1** and **2** could lead to cleavage of the backbone, and our initial target was a ligand with an extra CH_2 in the backbone to eliminate this

possibility. Phospholane-phosphite **5** is advantageously derived from a cheap *tropos* diol and a racemic phospholane and therefore was selected as our initial target. The synthesis of this ligand is shown in Scheme 1.

Scheme 1. Synthesis of phospholane-phosphite **5** with an extended backbone.

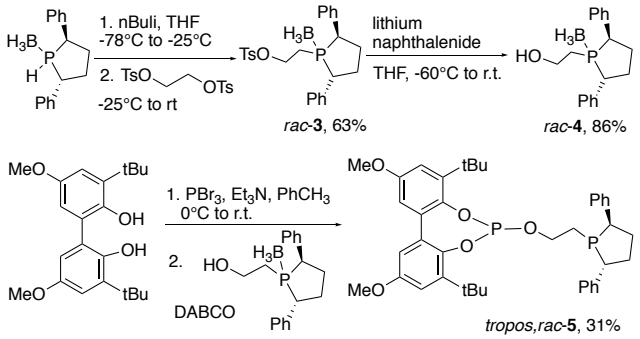

Preparation of the phospholane-containing fragment was achieved by deprotonation of the corresponding secondary phospholane with *n*-BuLi and reaction with ethane-1,2-diyl bis(4-methylbenzenesulfonate) to give, after deprotection, adduct **4**. The phosphite coupling to prepare **5** was achieved by forming the corresponding bromophosphite from the *tropos* diol, in the same way used in the preparation of BOBPHOS **1**,[7(d)] and this was reacted directly with precursor **4** in the presence of DABCO. Ligand (R_{ax},*R*,*R*)-**5b**, a single enantiomer variant of ligand **5**, was also prepared (Scheme 2), primarily to assist in reconciling NMR and HPIR data and will be discussed later.

Scheme 2. Synthesis of single enantiomer phospholane-phosphite **5b**.

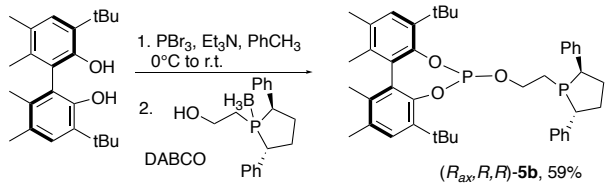

We have previously reported the use of fluorinated solvents such as octafluorotoluene and pentafluorophenyl *n*-octyl ether (PFPOE) to play a critical role in the enhanced regioselctivity towards *iso*-butanal using catalysts derived from ligands **1** and **2**.[5] A simpler non-volatile solvent would be preferable, so it was pleasing to find that the use of long-chain alkanes such as *n*-dodecane also worked well. Catalytic hydroformylation experiments in *n*-dodecane gave slightly lower selectivity than the hydroformylation in fluorinated solvents but superior relative to other common solvents as toluene. In all catalysis results in this paper, the catalysts were pre-activated by mixing [Rh(acac)(CO)$_2$] and ligand in the reaction solvent and syngas at 90°C. The time taken for this activation step was separately studied by *in situ* HPIR spectroscopy to ensure bands associated with the catalyst had grown to full intensity within the chosen activation times used in catalysis experiments. In this case, we found catalysts derived from ligand **5** to take much longer to form than those derived from ligand **1** (around 50 mins compared around 5 mins). The characterization of the pre-catalysts is discussed later. Tables 1 and 2 report TON frequencies at a predetermined time of 1 hour, except where noted. This was chosen since this provides a valid average TOF for the first part of the reaction; these TONs, are, with the exception of Table 2, entry 18 measured at below 50% conversion and all catalysts are stable beyond this time. Propene and syngas are consumed constantly up to this one-hour measurement, and hence these are single point measurement of experiments monitored continuously. If similar experiments are carried out at constant pressure with syngas added as the reaction proceeds, it is possible to measure the gas consumption until full conversion several hours later (see an example in ESI section 11). Rh/ (R_{ax},*R*,*R*)-**1**, afforded 70.2 % *iso* selectivity at 75 °C using *n*-dodecane as solvent (Table 1, entry 1), compared to 78.3% using octafluorotoluene.[5] We were delighted to find out that the *iso*-butanal selectivity of the Rh/ ligand **5** catalysts with the extended carbon linker was even greater than that of ligand **1** at 75°C, albeit with much lower reaction rate (Table 1, entry 2). Improved turnover frequencies (TOFs) were obtained at 90 and 105°C with *iso*-selectivity of around 70% and above: very unusually high for high temperature conditions (Table 1, entries 4 and 5). The results shown in Table 1 establish that the linker in phospholane-phosphite ligands such as **1** and **2** can be extended with no detrimental effect in the regioselectivity of the reaction, but an improvement under the conditions used. However, this does come at the cost of a drop in reactivity.

Table 1. Hydroformylation of propene using BOBPHOS and phospholane-phosphite **5**[a].

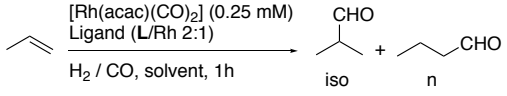

Entry	Ligand	T[°C]	Solvent	TON	Iso (%)
1[b]	**1**	75	dodecane	468	70.2
2[c]	**5**	75	dodecane	601	74.4
3[b]	**1**	90	dodecane	991	67.8
4	**5**	90	dodecane	139	72.5
5	**5**	105	dodecane	324	69.3
6	**5**	105	C_7F_8	222	69.9

(a) Catalyst preformed from [Rh(acac)(CO)$_2$] (5.12 x 10^{-3} mmol) and ligand (10.24 x 10-3 mmol) by stirring at 20 bar of CO/H_2 at 90°C for 45 min in the desired solvent (20 mL) and then increasing or decreasing the reaction T prior to running the reaction using a gas feed of propene/CO/H_2 1:4.5:4.5 ratio. Rh concentration = 2.52 x 10^{-4} mol dm^{-3}. Product determined by GC using 1-methylnaphthalene as an internal standard. The TON values actually correspond to average TOF values for the first part of the reaction, see discussion above. (b) Activation performed as above but at 50°C for 50 min (c) Reaction time 16h. Average TOF over 16h = 38.

The encouraging results obtained regarding the selectivity and preliminary experiments that showed Rh / **5** cata-

lysts to be stable over long periods led us to study further the effect of ligand backbone modification. It is well known that electron-withdrawing groups have an effect on the ligand making the phosphorus atom less basic and therefore leading to a decrease in the electron density of the metal center.[12] These more electron-deficient ligands should display an increased activity in the hydroformylation reaction.[1(a),(c)] Consequently we chose to include a strongly electron-withdrawing CF_3 group in the backbone (Scheme 3, ligands **9a** and **9b**).

Scheme 3. Synthesis of phospholane-phosphites bearing substitution in the backbone.

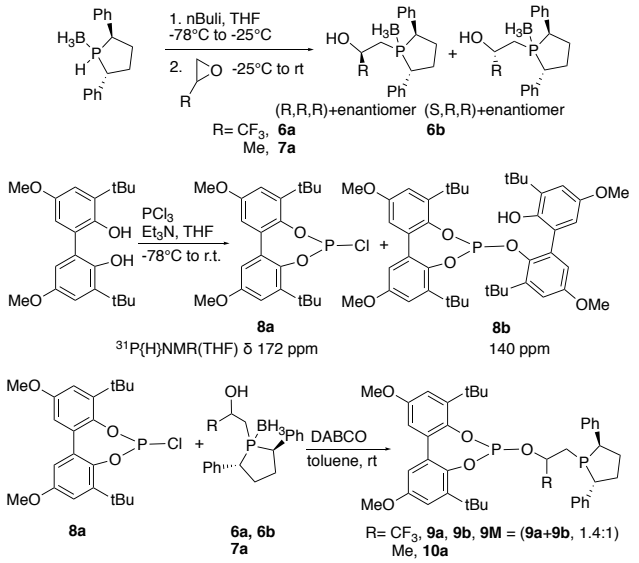

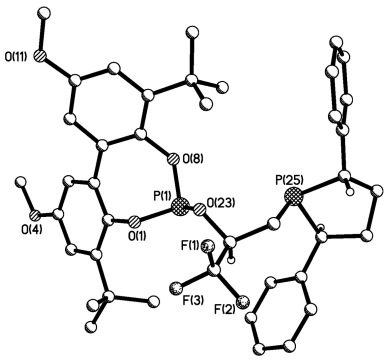

Figure 2. X-ray crystal structure of **9b**. Hydrogen atoms omitted for clarity except in stereocenters.

The first step in the synthesis of these ligands is the preparation of the alcohol precursors (Scheme 3, **6a** and **6b**). These precursors can be prepared in one step from commercially available racemic 2-(trifluoromethyl)oxirane. Regioselective attack of the resulting anion from deprotonation of the corresponding phospholane on the less substituted carbon of the epoxide afforded alcohols **6a** (major diastereomer) and **6b** (minor diastereomer) as a diasteromeric mixture in a 58:42 ratio estimated by $^{31}P\{^1H\}NMR$. These isomers could be separated by chromatography on SiO_2. The new ligands **9a** (obtained from major isomer **6a**) and **9b** (obtained from minor isomer **6b**) can be prepared as shown in Scheme 3). On this occasion the corresponding chlorophosphite from the *tropos* diol was formed in THF at low temperature, minimizing the formation of a byproduct, the unsymmetrical phosphite containing two *tropos* diol fragments ($^{31}P\{^1H\}NMR$, c.a. 140 ppm) that this diol is prone to form at higher temperatures.[13] The chlorophosphite was reacted directly with precursors **6a** or **6b** in the presence of DABCO to give the desired ligands **9a** and **9b**. In order to determine the absolute configuration of each diastereomer formed, a crystal structure determination of **9b** was obtained (Fig. 2). The configuration of ligand **9b** (in racemic form) is the (*S,R,R*) and (*R,S,S*) diastereomer. The relative stereochemistry of the corresponding precursors **6b** and **6a** are therefore assigned as the (*S,R,R*)/(*R,S,S*) pair, and (*R,R,R*)/(*S,S,S*) pair respectively.

Table 2. Hydroformylation of propene using new phospholane-phosphite ligands.[a]

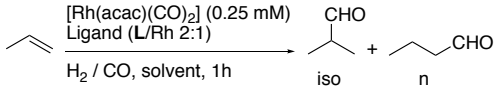

Entry	Ligand	T[°C]	Solvent	TON in 1 hr	*Iso* (%)
1	**9a**	75	dodecane	121	74.6
2	**9a**	75	C_7F_8	72	76.5
3	**9b**	75	dodecane	118	74.0
4	**9b**	75	C_7F_8	83	74.1
5	**9a**	90	dodecane	397	70.9
6	**9b**	90	dodecane	302	69.3
7	**9M**	90	dodecane	310	70.4
8[b]	**9M**	50	C_7F_8	256	79.2
9	**9a**	105	dodecane	782	67.2
10	**9b**	105	dodecane	663	65.1
11	**9M**	105	dodecane	675	66.5
12	**10a**	75	dodecane	48	75.9
13[c]	**10a**	75	C_7F_8	653	78.2
14	**10a**	90	dodecane	108	73.9
15	**10a**	105	dodecane	214	71.4
16	**11a**	75	dodecane	320	57.0
17	**11a**	90	dodecane	688	55.5
18	**11a**	105	dodecane	1148	53.7

[a]Catalyst preformed from $[Rh(acac)(CO)_2]$ (5.12×10^{-3} mmol) and ligand (10.24×10^{-3} mmol) by stirring at 20 bar of CO/H_2 at 90°C for the activation time for each ligand (**9a**, **9b** and **9M** 30 min, **10a** 100 min, **11a**, 20 min) in the desired solvent and then increasing or decreasing the reaction T prior to running the reaction using a gas feed of propene/CO/H_2 1:4.5:4.5 ratio. Rh concentration = 2.52×10^{-4} mol dm^{-3}. Product determined by GC using 1-methylnaphthalene as an internal standard. The TON values actually correspond to average TOF values for the first part of the reaction, see discussion on p 2 [b]Reaction time 17h. Average TOF over 17h = 18. [c]Reaction time 18h. Average TOF over 18h = 36.3.

The performances in the hydroformylation of propene in *n*-dodecane of these new fluorinated ligands were compared to the un-substituted ligand **5** (Table 2). We were pleased to find the desired leap in activity for both isomers **9a** and **9b** at 75°C, with a three-fold increase in average TOF (compare Table 1, entry 2 with Table 2, entries 1 and 3). Also, the level of *iso*-selectivity for these ligands was maintained at around of 74%. A similar behavior was also found when the reaction was run using octafluorotoluene, with a slightly better selectivity and a small drop in activity (entries 2 and 4). The improved reaction rate was maintained at the higher temperatures tested of 90 and 105°C while still displaying excellent regioselectivity for such high temperatures (entries 5, 6, 9 and 10). The fact both diastereomers, **9a** and **9b** display similar activity and selectivity opens up the possibility of preparing and using a diastereomeric mixture of **9a** and **b**, **9M,** without the need to previously separate precursors **6a** and **6b**. As expected, ligand **9M (9M** = **9a:9b** = 1.4:1), had a similar activity and selectivity to the individual isomers (Table 2, entries 7 and 11). A highest *iso*-selectivity of 79.2% was achieved with ligand **9M** in octafluorotoluene at 50°C (Table 2, entry 8). In order to confirm that the increase in activity from the catalyst derived from ligand **9M** is due mainly to electronic effects, the methyl substituted ligand **10a** was prepared and tested as a control. The methyl group would have very different electronic properties while having a reasonable similar steric bulk.[14] For reasons of simplicity, we used enantiopure precursor (*R,R,R*)-**7a** for the preparation of **10a**. The preparation of this ligand is described in Scheme 3. In terms of reactivity, **10a** generated a catalyst much slower than **9M** and of similar activity to **5** (Table 2, entries 12, 14 and 15). Higher *iso*-selectivity was also obtained in this case when the fluorinated solvent was used (Table 2, entry 13). These results support the positive effect on the reaction rate caused by the presence of the strongly electron-withdrawing CF_3 group in the backbone.

The modularity of these phospholane-phosphite ligands led us to modify the biphenol scaffold in order to make the phosphorus atom of the phosphite part less basic and therefore increase the reaction rate. Replacing *tert*-butyl groups in **5** and **9** with chlorine atoms would have a significant electronic effect, although Cl groups are much less bulky than *tert*-butyl groups, and the impact this would have was not known. This biphenol could be prepared in large amounts; 3,3',5,5'-tetrachloro-[1,1'-biphenyl]-2,2'-diol was prepared according to a known method by halogenation of biphenol with SO_2Cl_2.[15] This was readily converted to ligand *rac*-**11a** (Scheme 4).

Scheme 4. Synthesis of electron-deficient phospholane-phosphite **11a**.

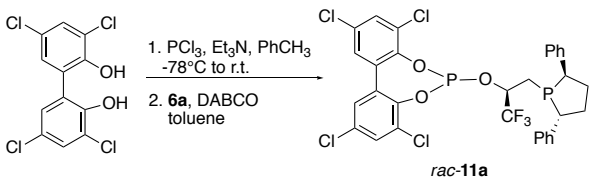

rac-**11a**

Electron-deficient precursor **6a** was chosen for the phosphite coupling to form ligand **11a**, which was prepared as previously described (Scheme 4). We were pleased to find out that the activity of this new catalyst was greater than that of Rh-**9M** at 75°C and much closer to the activity of Rh-BOBPHOS **1** (Table 2, entry 16), but there was a drop in selectivity to 57%. The ligand was still slightly branched-selective at higher temperatures (Table 2, entries 17 and 18) but far below the regioselectivity displayed from ligands **5**-**10**. It is reasonable to conclude that a substituent larger than chlorine is required in the *ortho*-position of the biphenol-derived part of the ligands. Overall, the catalysis studies establish that high *iso* selectivity is also possible using phospholane-phosphites that form a 6-membered chelate ring with rhodium.

A combination of *in situ* HPIR spectroscopy and variable temperature NMR spectroscopy was used to structurally characterize the catalyst resting state. This was also used to assess the stability of this resting state to heat. The rhodium hydrido dicarbonyl complex was deemed to have fully formed when the spectrum was constant and the spectra observed for [$RhH(CO)_2$(*tropos*,*trans*)-**5**)] over time as it forms is shown in Figure 3.

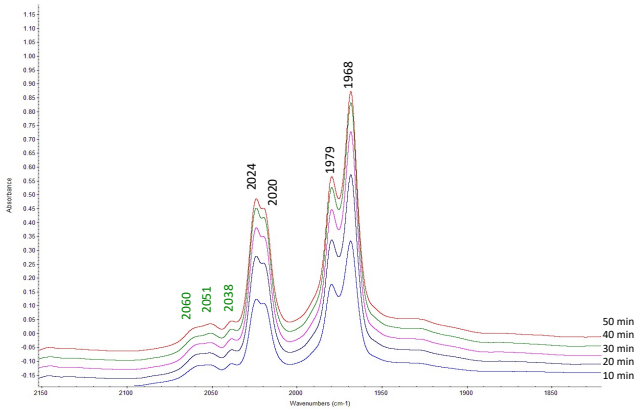

Figure 3. HPIR spectra of [$RhH(CO)_2$(*tropos*,*trans*)-**5**]. Conditions: Rh:L = 1:1.25 (C_{Rh}1 mM in dodecane), T = 90 °C, P= 20 bar, $CO:H_2$ 1:1. Full activation achieved after 50 min.

The presence of four main bands in the spectrum at 2024, 2020, 1979 and 1968 cm^{-1} suggests two coordination isomers in solution. This is in contrast with [$RhH(CO)_2$(R_{ax},*R,R*)-**1**)] which displays only two bands at 2029 and 1978 cm^{-1}. The asymmetric nature of the bands is consistent with an equatorial-axial *ea* coordination mode for one isomer.[8] Ligand **5** is a hybrid diphosphorus ligand with a *tropos* moiety, which opens the possibilities for the other isomer to be either: [I] Rh species with the ligand coordinated to equatorial-equatorial *ee* sites, or [II] an *ea* coordination mode with a different phosphorous in axial position or [III] it is also possible that the four bands observed correspond to the two possible *ea* rotational isomers analogous to *atropos R* and *S* enantiomers, that could be formed if there is restricted rotation once the *tropos* ligand is coordinated to Rh. Isomers with hydrides in equatorial position have never been observed in any type of complex of this type and are not considered. We have not found any evidence for unmodified Rh clusters that are the resting states after ligand decoordination (see ESI) To shed light on the coordination mode of **5**, another experiment was done using D_2/CO instead of H_2/CO. It has been observed that if any of the signals represents an *ee* species, the wave number of the CO stretch frequency will

change, due to removal of the interaction between $\nu_{(Rh-H)}$ and ν_{CO} from the CO ligand *trans* to it.[9] There are no shifts in the wave numbers showing that there are no CO in an apical position and therefore no isomer with *ee* conformation (Figure S5.2, ESI). The HPIR is therefore inconsistent with explanation [I] where there is an *ee* species present in solution. To distinguish between the other possibilities required the use of NMR spectroscopy, along with insights from the spectroscopic data from the other pre-catalysts.

Pre-catalyst [RhH(CO)$_2$(*tropos*,*trans*)-**5**)] was formed under syngas and also analyzed by NMR spectroscopy at ambient temperature (Scheme 5, see also ESI, section 5.3). The spectra obtained are very similar to those observed for [RhH(CO)$_2$((*R*$_{ax}$,*R*,*R*)-BOBPHOS)],[7(d)] and [RhH(CO)$_2$((*tropos,rac)*-**2**)],[5] and consist of a single set of signals, suggesting the presence of a single complex in solution under these conditions or a fast equilibrium amongst several species. The magnitude of $^2J_{P-H}$ (*phospholane*) coupling of 86 Hz is smaller than that observed for the aforementioned complexes and also to that of [RhH(CO)$_2$((*S*,*S*)-Ph-BPE)], ($^2J_{P-H}$ = 132 Hz at low temperature)[9(c)]. This is much larger than a *cis* coupling, which tends not to be observed, and much smaller than the values of $^2J_{P-H}$ when P is a phosphite (~220Hz) in axial position. This suggests that the major species has the phospholane in the axial position, as with ligands **1** and **2**.[10] Intermediate values of J_{P-H} at room temperature indicate a fast equilibrium mixture between the two *ea* (equatorial-axial) isomers or between *ea* and *ee* isomers.[10(b)(d)] Thus, the somewhat smaller value for $^2J_{P-H}$ (86 Hz) is likely to be an averaged value of two interconverting species: a major one in which the phospholane is axial and *trans* to the hydride and another *ea* species where it is equatorial and *cis* to the hydride, with a much smaller value of $^2J_{P-H}$.

It is known that mixtures of isomers of RhH(CO)$_2$(*P^P*)] complexes, when cooled to low temperatures, even if symmetric ligands are used, can lead to broadening of peaks before peaks can sometimes sharpen at very low temperatures: In one case of a RhH(CO)$_2$(phosphine-phosphite)] low T NMR has revealed the presence of two isomers in which different P atoms were *trans* to the hydride.[10(f)] Cooling the sample of [RhH(CO)$_2$(*tropos*,*trans*)-**5**)] down to –95°C, this time in CD_2Cl_2, did not show a separate resonance for either a species with equatorial-equatorial *ee* or an *ea* coordination mode, with the phosphite in axial position (see ESI). However, the value of $^2J_{P-H}$ for the phospholane, which is slightly larger in this solvent at room temperature (98Hz) did increase to 117 Hz, with the latter being close to a typical value for a phosphine in apical position *trans* to hydride (115-135 Hz). On its own this data is not quite sufficient to unequivocally assign the IR bands to either two rotational isomers (*pseudo* atropisomers) formed when the *tropos* ligand coordinated and rotation in the biphenol axis is frozen, or two *ea* species, but the latter certainly seems most feasible, with the other isomer likely to be populated to only a small extent and hence not observable in the low temperature NMR, and also not reducing the value of $^2J_{P-H}$ to a great extent.

The Rh complex of the single enantiomer variant of ligand **5**, i.e. (*R*$_{ax}$,*R*,*R*)-**5b,** made from a single atropisomer of an *atropos* biphenol (Scheme 3) was studied using HPIR spectroscopy (Figure 4).

Scheme 5. Characterisation of [RhH(CO)$_2$(*tropos,trans*)-**5**] by NMR.

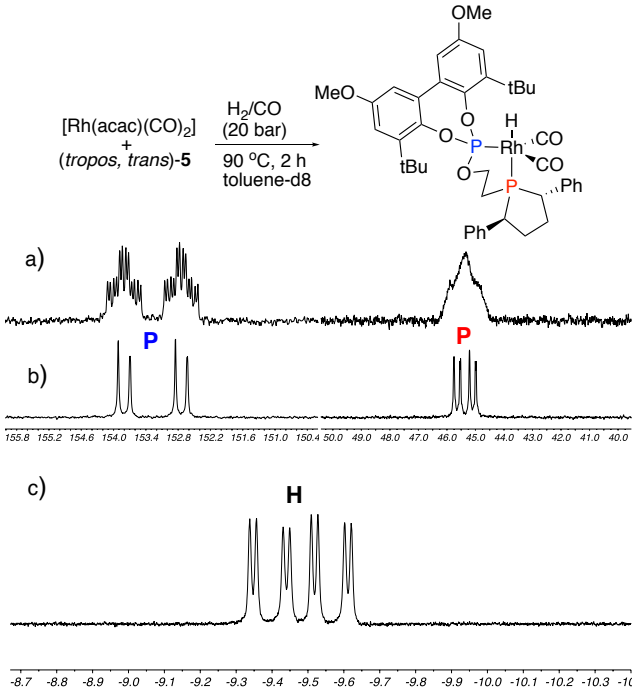

(a) ^{31}P NMR and (b) ^{31}P{H} NMR spectra (202 MHz, rt) showing the phosphite (P) and phospholane (P) regions. (c) ^{1}H NMR spectra (500 MHz, rt) showing the hydride region (H).

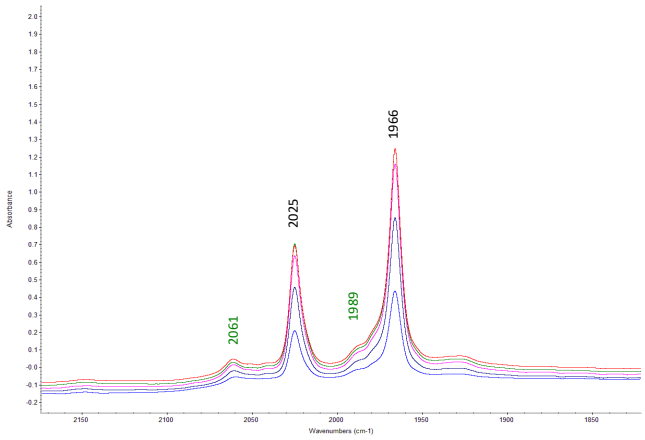

Figure 4. HPIR spectra of [RhH(CO)$_2$(*R*$_{ax}$,*R*,*R*))-**5b**]. Conditions: Rh:L = 1:1.25 (C_{Rh}1 mM in dodecane), T = 90 °C, P= 20 bar, CO:H_2 1:1. Full activation achieved after 70 min.

We initially considered that observing one pair of IR bands in this spectrum would support the explanation involving rotation isomers analogous to atropisomers in the HPIR spectra of [RhH(CO)$_2$(*tropos*,*trans*)-**5**)]. However, this would only be the case if the ambient temperature NMR coupling constants were similar in both complexes. In practice, while there are only two main bands in the HPIR

of [RhH(CO)$_2$(R_{ax},*R*,*R*)-**5b**)] (Figure 4), the NMR spectra shows a larger value for $^2J_{P\text{-}H}$ for the phospholane of 104 Hz. This data can therefore be explained by [RhH(CO)$_2$(R_{ax},*R*,*R*)-**5b**)] existing to a large extent as one *ea* isomer (with two main IR bands and $^2J_{P\text{-}H}$ close to typical values for phosphines in axial position trans to hydride). In contrast there is larger amount of a second *ea* isomer for [RhH(CO)$_2$(*tropos*,*trans*)-**5**)], and this is detectable by IR, and indirectly noticed in the low value for $^2J_{P\text{-}H}$ in the NMR spectra.

To increase our confidence as to whether two different rotational isomers (made possible by the *tropos* ligands becoming unable to rotate freely on coordination), different equatorial-axial or bis-equatorial isomers were most likely, DFT calculations were carried out on this aspect (B3PW91-D3/SDD(Rh)/6-311+G**/PCM$_{MeOH}$//RI-BP86-D3/SDD(Rh)/6-31G** level, see ESI for details). These started with the parent systems, (R_{ax},*R*,*R*)-**1**. The Rh catalysts derived from (R_{ax},*R*,*R*)-**1** have already been subject to detailed DFT study. [7d]

A number of regioisomers and conformers were located, which were all within a few kcal/mol of each other (see Fig 5). Computed (RI-BP86-D3 level) Rh-H and symmetric and asymmetric CO stretching modes were found in the region between ca. 1950 – 2065 cm^{-1} (see Tables S9.2 & S9.6 in ESI), in good qualitative agreement with experiment (e.g. Figure 4) and in line with accuracies typical for this and related DFT levels.[16] The calculations also predict that when hydride is swapped for deuterium, only the *ee* isomer exhibits significant changes. This latter aspect has been observed in the IR spectra of Rh complexes of this type derived from other ligands.[9] This is because in this case H is trans to CO (see sketch in Fig. 5 top), and the normal modes contain contributions from both Rh-H and CO stretches (see Figure S9.2 in the ESI), so that switching to Rh-D also imparts noticeable changes in the CO stretching frequencies. We now compare the energetics of the *ea* isomer with phosphite axial, from herein termed eq-ax(ax-P(OR)$_3$), the *ee* isomer, and the *ea* isomer with phospholane-*trans*-H [eq-ax(ax-PR$_3$)] for (R_{ax},*R*,*R*)-1 (Fig. 5). In addition we compared these to the other diastereomer, (S_{ax},*R*,*R*)-**1**, on the basis that the (R_{ax},*R*,*R*)- and (S_{ax},*R*,*R*)-diastereomers represent the two conformations the *tropos* biphenols might adopt in Rh pre-catalysts derived from *tropos-rac*-**2**. The calculations agree with experiment since for the Rh pre-catalysts derived from (R_{ax},*R*,*R*)-**1**, the *ea* isomer experimentally observed is significantly lower in energy than other isomers. The other diastereomer Rh/(S_{ax},*R*,*R*)-**1** is predicted to be 3.7 kcal above the predicted catalyst resting state for [RhH(CO)$_2${(R_{ax},*R*,*R*)-**1**}]. This is a significant energy difference and consistent with the ligand with a *tropos* biphenol, *tropos-rac*-**2**, preferring to adopt a biphenol conformation more similar to (R_{ax},*R*,*R*)-**1**, than (S_{ax},*R*,*R*)-**1**. Reference 5 discusses Rh catalysts derived from a *tropos* diol but with an enantiomerically pure (*R*,*R*)-phospholane giving the same sense of enantioselectivity and enantiomer ratios relatively similar to using Rh/(R_{ax},*R*,*R*)-**1** catalysts, which is consistent with this.

The calculations were then adapted to the more configurationally flexible 6-membered rings that the Rh pre-catalysts derived from ligands such as **5** adopt. The energies of the isomers for [RhH(CO)$_2$(R_{ax},*R*,*R*)-**5b**)] show that while the earlier discussed *ea* isomer with phospholane-*trans*-H, [eq-ax(ax-PR$_3$)] is favoured, the energy for the ee isomer becomes closer (reducing from + 4.6 to + 2.1 kcal/mol), consistent with the larger bite angle of **1** vs. **5**/**5b**, and while not predicted to be a major isomer, eq-eq is getting closer in energy. The other possible *ea* isomer, eq-ax(ax-P(OR)$_3$, is predicted to be significantly less stable in energy. While this does agree quite well with the experimentally observed IR spectra showing only two main bands for [RhH(CO)$_2$(R_{ax},*R*,*R*)-**5b**)] (Fig. 4), the large energy difference did leave us wondering how to reconcile the experimental support for the eq-ax(ax-P(OR)$_3$ isomer for very similar complex, [RhH(CO)$_2$(*tropos*,*trans*)-**5**)]. However, when the energies of the Rh resting states for the diastereomeric ligand (S_{ax},*R*,*R*)-**5b** were calculated, they reveal significant differences.

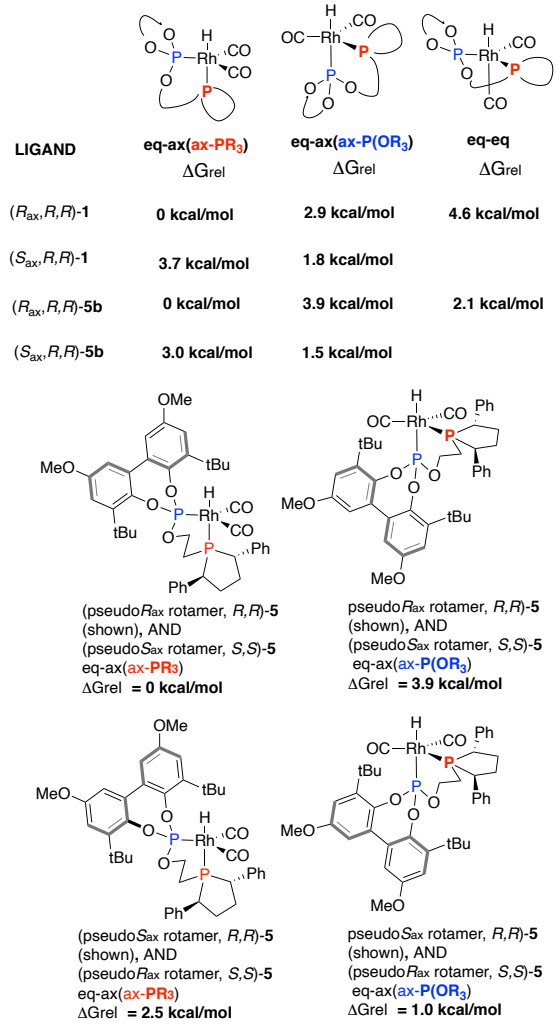

Figure 5. Computed (B3PW91-D3 level) relative free energies of selected complexes with **1** and **5** (in kcal/mol at room temperature, relative to the most stable respective isomer).

The most significant and striking difference in this system is that on going from ligand (R_{ax},*R*,*R*)-**5b** to (S_{ax},*R*,*R*)-**5b** the other *ea* isomer, eq-ax(ax-P(OR)$_3$, changes from being 3.9 kcal/mol higher in energy to just 1.5 kcal/mol higher in

energy [w.r.t. the most stable *ea* isomer, eq-ax(ax-PR_3) , for [RhH$(CO)_2$(*R*$_{ax}$,*R*,*R*)-**5b**)]. Moreover, this isomer is more stable than the eq-ax(ax-PR_3) isomer for (*S*$_{ax}$,*R*,*R*)-**5b** (1.5. kcal/mol vs 3.0 kcal/mol. In light of these findings, the surprising large difference in the spectra between [RhH$(CO)_2$(*R*$_{ax}$,*R*,*R*)-**5b**)] and [RhH$(CO)_2$(*tropos*,*trans*)-**5**)] may well be due to the latter being able to form another rotational isomer, similar to [RhH$(CO)_2$(*S*$_{ax}$,*R*,*R*)-**5b**)], and that this conformer only binds in the *ea* mode with phosphite *trans* to hydride. A final calculation that lends extra weight is a calculation on the possible rotational isomers that *tropos-rac*-**5** could adopt (see ESI for details). While this is a molecule with a large number of possible conformations, and there may be slightly higher uncertainty on the specific values, once again, the rotational isomer analogous to (*S*$_{ax}$,*R*,*R*)-**5b** prefers to form a [eq-ax(ax-$P(OR)_3$] isomer (1.0 kcal/mol) more than a [eq-ax(ax-PR_3)] isomer (2.5 kcal/mol), and both of these are higher in energy than the [eq-ax(ax-PR_3)] isomer for the rotational isomer that is analogous to (*R*$_{ax}$,*R*,*R*)-**5b** (0 kcal/mol). In summary, we conclude that for the *tropos* ligands, the [eq-ax(ax-$P(OR)_3$] isomer becomes feasible for one rotational isomer that is more akin to the mismatched isomer of ligands derived from *atropos* biphenols, but the main *ea* isomer [eq-ax(ax-PR_3)] is not accessible for the other rotational isomer. An *ee* isomer is a possibility with the ligands reported here with 6-membered chelate rings, but seems unlikely for ligands **1** and **2**. Since these most striking trends are based on calculated energy differences of at least 1.5 kcal/mol, we suggest they qualitatively predict the relative energies of the relevant isomers for [RhH$(CO)_2$(*R*$_{ax}$,*R*,*R*)-**5b**)]

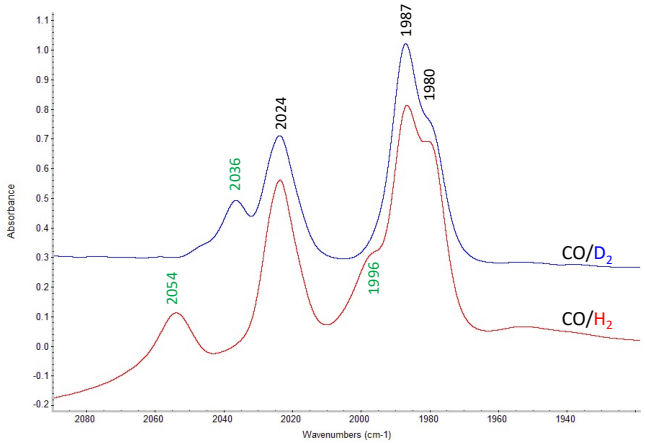

Figure 6. HPIR spectra of [RhH$(CO)_2$(*tropos*,*trans*)-**9a**] (bottom) and RhD$(CO)_2$(*tropos*,*trans*)-**9a**] (top). Conditions: Rh:L = 1:1.25 (C_{Rh}1 mM in dodecane), T = 90 °C, P= 20 bar, CO:H_2 1:1 or CO:D_2 1:1, 1h.

Analysis of [RhH$(CO)_2$(*R*$_{ax}$,*R*,*R*)-**9a**)] using HPIR and low temperature NMR spectroscopies increases confidence in the assignments above. This ligand shows different coordination behaviour. Here, the HPIR spectra (Fig. 6) shows additional bands from those assigned to the *ea* isomer with phospholane-*trans*-H (1980 and 2024 cm^{-1}).

Since there is significant similarity to different *ea* isomers and even the IR spectrum of the *ee* isomer is in broadly the same area, it is hard to assign much further, so the experiment using D_2/CO was repeated for this ligand. In the earlier case, this essentially showed a very, very similar spectrum with no peak shifts. However, for **9a**, there are significant differences between the HPIR spectra. While in practice, this did not produce a spectrum that is straightforward to assign bands exclusively to *ee* and *ea* isomers, the fact there is significant change is not in doubt, and most likely some of the *ee* band previously observed at 1996 cm^{-1} has moved underneath the 1980-1990 cm^{-1} region for the deuterated complex, while the stretch at 2054 cm^{-1} has moved to 2036 cm^{-1}. There is therefore evidence in this case that an *ee* isomer with H-*trans*-CO being present in a significant amount. This was then confirmed quite clearly in NMR experiments. Scheme 6 shows the ^{1}H NMR as the temperature is lowered to –95 °C. The solvent had to be changed to CD_2Cl_2 to observe peaks resolving into separate signals even at this very low temperature. The spectrum at –95 °C displays three separate multiplets that take a form consistent with two *ea* isomers and one *ee* isomer. The furthest upfield peak at – 11.2 ppm can be assigned to the *ee* isomer since all couplings between H and P are *cis,* and hence small, as is $^1J_{H\text{-}Rh}$. The signal at -9.9 ppm has a $^2J_{H\text{-}P}$ of 116 Hz, which is in the same type of magnitude we have observed before when phospholanes are *trans* to hydride in the axial position. Other couplings $^2J_{H\text{-}P}$ for the phosphite *cis* to H and $^2J_{H\text{-}Rh}$ are too small to be resolved as expected. The peak at -10.4 has two significant couplings, one with a $^2J_{H\text{-}P}$ of 169 Hz and one with a $^2J_{H\text{-}P}$ of 50 Hz. This larger coupling constant can be assigned to one coupling being predominantly from a phosphite in axial position *trans* to hydride. However, this is somewhat smaller than a pure a $^2J_{H\text{-}P}$ for a phosphite trans to hydride as discussed for the Rh-BINAPHOS complex.[10f] The value of a $^2J_{H\text{-}P}$ of 50 Hz for the phospholane *cis* to the hydride is also larger than would be expected for a *cis* H-P coupling constant.

It can be concluded that even at the technical limit of this low temperature experiment, there is still some interconversion between these isomers, leading to slightly larger *cis* coupling and slightly smaller *trans* coupling, although the resolution of these 3 peaks is sufficient to assign them unambiguously. This direct observation of coupling constants is in agreement with observations discussed earlier, and shows that all three of these isomers are relatively similar in energies. This is in contrast to what is observed for Rh pre-catalysts formed from either (*R*$_{ax}$,*R*,*R*)-**1** and *tropos-rac*-**2**, and is primarily an effect of increasing the carbon chain between the donor atoms. The branched selectivity displayed by Rh catalysts derived from (*R*$_{ax}$,*R*,*R*)-**1** is unique for bidentate ligands except for these new variants reported here, and has been the subject of an extensive mechanistic investigation.[7d] For these ligands we cannot entirely rule out an entirely different catalytic cycle starting from one of these other *ea* or *ee* isomers that are relatively close in energy for these 6-membered chelate rings. However, it is not logical to assume a totally different catalytic cycle predominates that is also unique in giving high branched selectivity. We therefore expect the catalytic cycle to be one using the *ea* phospholane-*trans*-H species as pre-catalyst.

Scheme 6. Low temperature NMR spectroscopy investigation of the coordination mode of [RhH(CO)$_2$(*tropos,trans*)-**9a**]

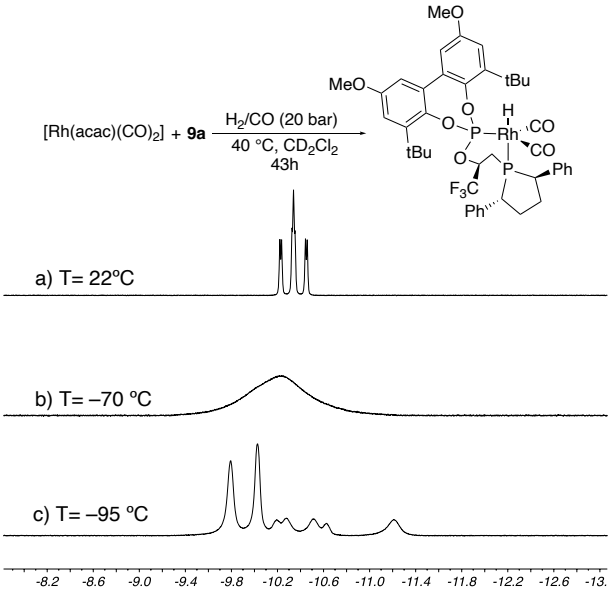

^{1}H-NMR (500 MHz, CD_2Cl_2) spectrum of [RhH(CO)$_2$(*tropos,rac*-**9a**)] showing the hydride region at rt (a). δ -10.34 (ddd, $^2J_{P\text{-}H}$ = 59.3 Hz, $^2J_{P'\text{-}H}$ = 53.0 and $^1J_{Rh\text{-}H}$ = 7.5 Hz). (b, –70 °C) δ -10.22 (br s). (c, –95 °C) δ -9.91 (br d, $^2J_{P\text{-}H}$ = 116.2 Hz), -10.40 (br dd, $^2J_{P\text{-}H}$ = 169 Hz, $^2J_{P'\text{-}H}$ = 50), 11.22 (br s).

A prime motivation for this study was to identify ligands that would have stability far beyond the 1-16 hours typically used to carry out a laboratory scale hydroformylation experiment. Phospholane-phosphite ligands such as **1** and **2** are hybrid ligands with several different possibilities for decomposition including hydrolysis, oxidation and others.[6,8(d),11] After the encouraging results obtained in propene hydroformylations at high temperatures with ligand **5,** [RhH(CO)$_2$(*tropos*,*trans*)-**5**)] was formed at the higher temperature of 105°C instead of 90°C; after 4 hours the spectrum is unchanged and similar to that already described. The earlier catalyst, [RhH(CO)$_2$(*R$_{ax}$,R,R*)-**1**] shows the formation of some extra bands in the IR spectra within 3 hours (see ESI).

Two parallel experiments were performed in the same autoclave at 90 °C and 20 bar of syngas in d^8-toluene. First, to check the formation of both [RhH(CO)$_2$(**L**)] complexes, they were analyzed after 2 h. ^{31}P{H}NMR showed the presence of both complexes in solution (ESI, Section 5). Then, the same experiments were done but the samples were analyzed 18h later. Rh/ **1** showed low stability and after 18h, none of the original rhodium hydrido dicarbonyl complex was observed in solution (ESI, Figure S5.2). On the other hand, [RhH(CO)$_2$(*tropos*,*trans*)-**5**)] was present as the main species in solution, albeit accompanied by some minor unidentified Rh complex. [RhH(CO)$_2$(*tropos*,*trans*)-**5**)] shows a much greater stability than Rh/ **1**. Since the main difference between ligands **1** and **5** is the extended backbone in ligand **5**, these results suggest that the lack of stability of [RhH(CO)$_2$(**1**)] is mainly due to the P,O acetal structure present in in this ligand. Next, the same sample of [RhH(CO)$_2$(*tropos*,*trans*)-**5**)] used in the NMR experiment was diluted in *n*-dodecane and used to record a HPIR spectrum at r.t (ESI, section 5.3.3). The spectrum obtained is similar to that shown in Figure 2 but with d8-toluene obscuring some parts of the spectrum, allowing us to correlate the HPIR and NMR data to the same species.

The stability at the higher temperature of 105°C for the corresponding pre-catalysts [RhH(CO)$_2$**L**)] of the four new ligands with substitution in the backbone **(9a, 9b**, **10a**, and **11a**) was also studied using HPIR spectroscopy (ESI, Section 7). Especially harsh conditions were chosen for this study to try to promote decomposition; although it was recognized that a catalyst could be very stable at typical reaction temperatures of 90 °C but decompose rapidly above a certain threshold, it was felt that high stability under these conditions would bode well for longer experiments at lower temperatures in the future. While HPIR could distinguish the formation of new species, the tendency for band overlap and broadening means it is only a qualitative tool to identify trends. After one day at 105 °C, the IR spectra from Rh precatalysts generated from either ligands **10a** or **11a** does not resemble that obtained using freshly generated [RhH(CO)$_2$(**10a**)], or [RhH(CO)$_2$(**11a**)] (ESI, section 7). However, the spectra obtained for [RhH(CO)$_2$(**9a**)] is similar to that observed from a freshly generated sample (ESI, Fig. S7.3). Indeed: there is no significant change in the spectra for [RhH(CO)$_2$(**9m**)] even after 72 hours (Fig. 7). This experiment proves that the under the conditions it was ran there is very, very little catalyst decomposition. It is certainly possible that trace amounts of the unmodified catalysis or decomposed Rh/ ligand species could be forming below the detection limit of this experiment, and it would be expected that eventually almost all Rh/P ligand catalysts will decompose. However, if these are present, we have been unable to detect them using methods that we have previously used to unmodified Rh catalysts resting states.[4c]

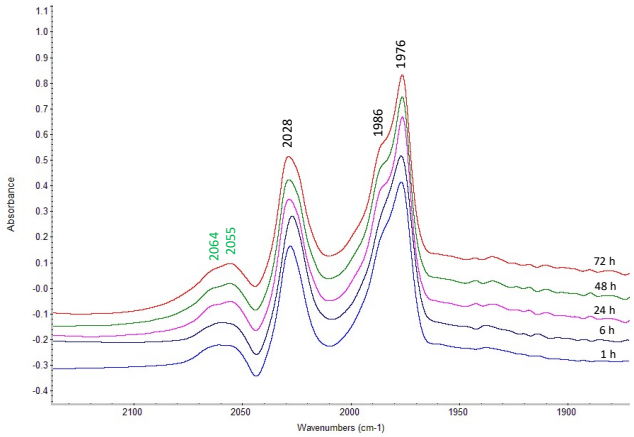

Figure 7. HPIR spectra of [RhH(CO)$_2$(*tropos*,*trans*)-**9m**]. Conditions: Rh:L = 1:2 (C_{Rh}1 mM in dodecane), T = 105 °C, P= 20 bar, CO:H_2 1:1.

It is not possible to link specific structural features within the ligands **10a**/**11a** to stability in these cases to a great extent. However, it is perhaps worth noting that *ortho-tert-*

butyl substituted aryl phosphites have previously been considered to be less prone to hydrolysis than other aryl phosphites,[6a,d] and it may be that *ortho*-chloro-aryl phosphites cannot replicate this bulky *ortho* substituent effect. Since Rh catalysts derived from **9a** give far better selectivity and productivity than Rh/ **10a** or Rh/ **11a**, it was pleasing to find very good high temperature stability for Rh/ **9a**, and further experiments using NMR spectroscopy to assay the long stability of the 'best' catalyst identified in this work, [RhH(CO)$_2$(**9a**)] were carried out.

We initially prepared the complex in toluene-d8 and analyzed it by NMR in the same manner as described for ligand **5**, then we prepared the complex and heated it in *n*-dodecane at 90°C and 20 bar of syngas for a whole week (Scheme 7 and ESI, Section 5.2). The sample was then analyzed at ambient temperature and pressure of syngas. We were very pleased to find out that [RhH(CO)$_2$(**9a**)] was the only species detected by NMR. This complex showed a remarkable thermal stability under these conditions, confirming the results obtained by HPIR spectroscopy.

Scheme 7. Long term stability study of [RhH(CO)$_2$(*tropos,trans*)-**9a**] by NMR.

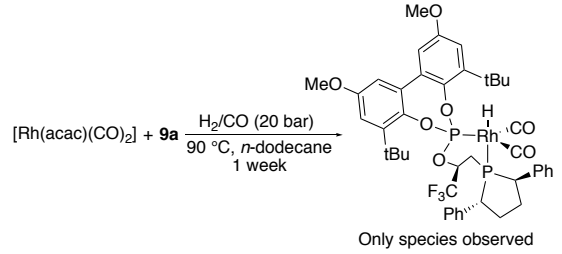

Furthermore, the stability of [RhH(CO)$_2$(**9M**)] was also checked in the presence of aldehydes. The hydroformylation of propene was carried out using similar conditions described in Table 2, but on this occasion, after the activation period, we added *n*-hexanal (5 mmol) and kept the mixture in the reactor stirring at 80°C and 20 bar of syngas for 17h before running the reaction with propene. We were pleased to find that the catalyst performed in a similar way to that in the run without 17 hours of "aging" with *n*-hexanal, affording the product with a TON of 327 and an *iso* ratio of 69.4% (compare with Table 2, entry 7). The following further experiments were conducted to confirm stability under industrially relevant conditions. A hydroformylation experiment was carried out in a larger vessel until propene was consumed; this delivered a TON of 2700 (67.8 % *iso*) after 19 h at 90 °C (see ESI, section 2.3). Finally, ligand *tropos-trans*-**5** was subjected to an industrial stability protocol (see ESI, section 10 for details) over 4 days between 90 and 105 °C with no signs of catalyst decomposition being detectable during this period as evidenced by consistent rates and selectivity after 4 days of operation. Nearly 3Kg of aldehydes were produced with a total TON of over 268000 when the experiment was discontinued.

CONCLUSIONS

Prior to this study, Rh catalysts derived from *racemic tropos* ligand **2**, or BOBPHOS **1**, delivered unprecedentedly high selectivity for *iso*-butanal with useful rates in the hydroformylation of propene in fluorinated solvents; as reaction temperatures were increased above around 85 °C, some catalyst degradation was observed. Under hydroformylation conditions, this was not as simplistic as a simple hydrolysis of one bond in a ligand, but under reactions conditions, leading to a very complex mixture, none of which being the normal catalysts resting state for thee species (see SI). The stability of hydroformylation catalysts is an important issue,[1c, 11,17] since practical applications to make relatively high-volume cheaper chemicals like simple linear aldehydes need a long catalyst lifetime. Recently very, very stable Co catalysts have been disclosed,[17] but various Rh/P-ligand systems have been applied commercially that show sufficient stability, and the target here was for catalysts to be primarily unchanged after several days. The new ligand reported here include *iso* selective catalysts that show no signs of degradation after several days to one week; they are anticipated to have a much longer lifetime as a useful catalyst, and the stability study carried out in a vapour stripped reactor was discontinued after several Kg of aldehydes were produced, having passed the test, not reached the end of the catalysts lifetime. The extended backbone is a significant aspect that confers greater stability, but also has a significant impact on the donor properties of the ligands, which then impacts on both reaction rate and time to activate. HPIR analysis of [RhH(CO)$_2$(**11a**)], the most active catalyst, showed two main bands at 2036 and 1990 cm^{-1} and when compared with the rest of ligands with an extended backbone studied here (Table 3), we can see that there is a correlation between activity and the wavenumber of the CO stretching bands: the complexes with the stretch at highest wavenumbers affording the most active catalysts (**9a**, **9b** and **11a**) while the least active catalyst, the complex generated from **10a**, displays CO stretches at the lowest wavenumbers.

The activation time to form the pre-catalysts increases as the values for the CO stretches are observed at lower wavenumber. Pre-catalyst [RhH(CO)$_2$(**11a**)] was formed at 90°C and 20 bar of syngas, taking just 20 min to achieve full activation (ESI), which was the shortest time for the new ligands presented in this work. [RhH(CO)$_2$(*tropos,trans*)-**9a**)] and [RhH(CO)$_2$(*tropos*,(*trans*)-**9b**)] takes 30 minutes at 90°C and 20 bar of syngas, faster than the 50 min needed for Rh/ **5** under the same conditions. The activation time to form the corresponding catalytic resting state [RhH(CO)$_2$(*tropos*,(*R,R,R*)-**10a**)] at 90°C and 20 bar of syngas was much longer, taking 100 min to achieve full activation (ESI). Activation of the catalysts is a significantly different reaction to hydroformylation, encompassing coordination, and then hydrogenolysis of the acac ligand, followed by uptake of CO. We believe the initial coordination is very fast, and have previously observed the formation of [Rh(acac)(BOBPHOS)] to occur as soon as you can run an NMR spectra, but as pointed out by a reviewer, the possibility exists that partial coordination occurs for these ligands and then it is quite slow to complete the formation of the chelate, and this might have a strong ligand efect. The reason we favour is the likely formation of a dihydrogen complex, or an intermediate/transition state with a dihydrogen-Rh interaction that is deprotonated by the acac

ligand, and a stronger pi-acceptor ligand makes the dihydrogen more easily deprotonated.

Table 3. HPIR main absorptions observed for the [RhH(CO)$_2$L] species presented in this work.

Complexes	ν (ea) (cm^{-1})
[RhH(CO)$_2$**1**]	2029, 1978
[RhH(CO)$_2$**5**]	2024, 2020, 1979, 1968
[RhH(CO)$_2$**5b**]	2025, 1966
[RhH(CO)$_2$**9a**]	2024, 1987, 1980
[RhH(CO)$_2$**9b**]	2030, 1985, 1975
[RhH(CO)$_2$**10a**]	2018, 1979, 1972
[RhH(CO)$_2$**11a**]	2036, 1990

The longer backbones had a significant impact on the speciation of the pre-catalysts, which often existed as several isomers. Aided by having a series of ligands, it was possible to use *in situ* HPIR spectroscopy in the presence of both H_2/CO and D_2/CO, combined with low temperature NMR and DFT calculations to assign the structure of the catalyst resting states.

The phospholane phosphites with extended backbone, such as ligand **5** lead to more stable catalysts, and we also report that cheaper *n*-dodecane can be used as solvent which leads to almost as high *iso* selectivity as fluorinated solvents earlier found to critical for this alkene, and significantly better than those observed in toluene. Rh catalysts derived from ligand **5** showed remarkable *iso*-selectivities, better than those from Rh/ **1**, or any other known catalyst at high temperatures (75-105°C) but with much lower TOFs. Ligands **9a** and **9b**, bearing a strongly electron-withdrawing CF_3 group produced highly stable *iso*-selective hydroformylation catalysts with improved TOFs compared to **5**.

It would still be desirable to discover more *iso*-selective propene hydroformylation catalysts, with desirable properties being very inexpensive synthesis, high *iso*-selectivity, stability at 90-110 °C, and giving activity that matches very active Rh/**1** catalysts; Further research on *iso*-selective hydroformylation of propene is still desirable.

EXPERIMENTAL SECTION

General information. All reactions were performed under an inert atmosphere of nitrogen or argon using standard Schlenk techniques, unless otherwise stated. All glassware used was flame-dried. Dry and degassed solvents were obtained from a solvent still or SPS solvent purification system. Commercially purchased anhydrous solvents were degassed before use by the freeze-pump-thaw method or by purging with inert gas. Triethylamine was dried and degassed before use. All chemicals, unless specified were purchased commercially and used as received. CO/H_2 and propylene/CO/H_2 (10/45/45%) were obtained premixed from BOC. NMR spectra were recorded on a Bruker Avance 300, 400 or 500 MHz instrument. Proton chemical shifts are referenced to internal residual solvent protons. Carbon chemical shifts are referenced to the carbon signal of the deuterated solvent. Signal multiplicities are given as s (singlet), d (doublet), t (triplet), q (quartet), m (multiplet) or a combination of the above. Where appropriate coupling constants (*J*) are quoted in Hz and are reported to the nearest 0.1 Hz. All spectra were recorded at r.t. (unless otherwise stated) and the solvent for a particular spectrum is given in parentheses. NMRs of compounds containing phosphorus were recorded under an inert atmosphere in dry and degassed solvent. Gas chromatography was performed on an Agilent Technologies 7820A machine. Mass spectrometry was performed on a Micromass GCT spectrometer, Micromass LCT spectrometer, Waters ZQ4000, Thermofisher LTQ Orbitrap XL or Finnigan MAT 900 XLT instruments. Flash column chromatography was performed using Merck Geduran Si 60 (40-63 μm) silica gel. Thin layer chromatographic (TLC) analyses were carried out using POLYGRAM SIL G/UV254 or POLYGRAM ALOX N/UV254 plastic plates. TLC plates were visualized using a UV visualizer or stained using potassium permanganate dip followed by gentle heating.

General Procedure for rhodium-catalysed hydroformylation of propene. CAUTION: Carbon monoxide is toxic and highly flammable. All manipulations are carried out in a well-ventilated fumehood with carbon monoxide detectors in place to detect for leaks and appropriate signage and communication about CO usage with colleagues. Hydroformylation reactions of propene were performed in a Parr 4590 Micro Reactor fitted with a gas entrainment stirrer; comprising of holes which gives better gas dispersion throughout the reaction mixture. The vessel had a volume capacity of 0.1 L, an overhead stirrer with gas entrainment head (set to 1200 r.p.m.), temperature controls, pressure gauge and the ability to be connected to a gas cylinder. Ligand (6.40 μmol (Rh:L 1:1.25) or 10.24 μmol (Rh:L 1:2)) was added to a Schlenk tube, which was then purged with nitrogen (or argon). The internal standard 1-methylnaphthalene (0.1 mL) was then added. The mixture was dissolved in a stock solution of [Rh(acac)(CO)$_2$] in toluene (2 mg/mL, 0.66 mL, 5.12 μmol of [Rh(acac)(CO)$_2$]), followed by the addition of the designated solvent (19.34 mL). The solution was transferred *via* syringe to the pressure vessel (which had been purged with CO/H_2) through the injection port. CO/H_2(1:1) (20 bar) was added and the heating jacket set to the desired temperature while stirring. Once the desired temperature was reached, the reaction was stirred for the required time to fully activate the catalyst. Then pressure was slowly released and repressurized with propene/CO/H_2. The reaction was then run for the time specified in the tables. After this time, stirring was stopped and the reaction was cooled by placing the vessel in a basin of cold water. The pressure was released, and the crude sample was analyzed immediately by GC (in toluene). The GC method was run on a HP-5 Agilent column; with length 30 m, diameter 0.250 mm and film 0.25 μm. The oven was initially held at 25 °C for 6 minutes, and then increased to 60 °C at a rate of 10 °C per minute. The ramp was then increased to 20°C per minute until the temperature reached 300°C. The products could be identified with the following retention times; *iso*-butyraldehyde (1.02 min); *n*-butyraldehyde (1.15 min) and 1-methylnaphthalene (13.50 min). The GC was calibrated for propene hydroformylation using (1-methylnaphthalene) as an internal standard. Both the linear (*n*-butyraldehyde) and branched (*iso*-butyraldehyde) products were calibrated against the internal standard and against each other. The branched selectivities of some reactions (especially those in fluorinated solvents) were further verified by ^{1}H NMR spectroscopy.

General procedure for monitoring the complexation of ligands using HPIR spectroscopy. CAUTION: Carbon monoxide is toxic and highly flammable. All manipulations are carried out in a well-ventilated fumehood with carbon monoxide detec-

tors in place to detect for leaks and appropriate signage and communication about CO usage with colleagues The HPIR spectroscopy pressure vessel was purged with CO/H_2 three times and then *n*-dodecane (22 mL) was injected to the pressure vessel. The heating jacket set to 90 °C (or the desired temperature) while stirring. Once the required temperature was reached, the vessel was pressurised at 20 bar of syngas and a background spectrum was recorded (1024 scans). [Rh(acac)$(CO)_2$] (0.06 mmol) and ligand (0.075 mmol (Rh:L 1:1.25)) was added to a flame dried schlenk tube, which was then purged with nitrogen (or argon). *n*-dodecane (8 mL) was added to dissolve the rhodium precursor and ligand and stirred for 10 minutes. The reaction mixture was then transferred *via* syringe to the pressure vessel (which had been depresurized before addition) through the injection port, pressurized with CO/H_2 (20 bar) and sampling initiated, 128 scans per spectrum. Precatalyst formation was then monitored by IR.

Full Experimental details and characterization are available in the ESI.

4,8-di-tert-butyl-6-(2-((trans)-2,5-diphenylphospholan-1-yl)ethoxy)-2,10-dimethoxydibenzo[d,f][1,3,2]dioxaphosphepine, ***5***. 3,3'-di-*tert*-butyl-5,5'-dimethoxy-[1,1'-biphenyl]-2,2'-diol (0.228 g, 0.637 mmol) was placed in a Schlenk tube and suspended in 3 mL of toluene. NEt_3 (0.266 mL, 1.911 mmol) was added and the resulting solution cooled in an ice bath. PBr_3 (0.091 mL, 0.956 mmol) was added dropwise to the reaction mixture, which was then removed from the ice bath and stirred for 16 h. The suspension was filtered *via* cannula under an inert atmosphere, and the filtrate was evaporated using a Schlenk line and dried under vacuum to remove any residual PBr_3. The crude $^{31}P\{^1H\}$ NMR (202.4 MHz, C_6D_6) spectrum showed two peaks at δ 189.4 ppm, corresponding to the bromophosphite and a second peak at 140.6, corresponding to a byproduct, in 3:1 ratio. The product was used in the next step without further purification. To a Schlenk flask containing a solution of the bromophosphite from the previous step in toluene (3 mL) was added a solution of (*trans*, *rac*)-phospholane adduct *rac*-**4** (0.161 g, 0.541 mmol) in toluene (4 mL) followed by a solution of 1,4-diazabicyclo-[2,2,2]-octane (DABCO) (0.607 g, 5.41 mmol, 10 eq.) in toluene (3 mL). The reaction mixture was then allowed to stir at room temperature overnight (19 h). The resulting suspension was filtered through silica gel (previously dried overnight in an oven) under an inert atmosphere, using dry toluene to compact and wash the SiO_2 after filtration. The resulting solution was evaporated under reduced pressure to afford a white foamy solid. Purification of (*tropos*, *trans*)-**5** was achieved by recrystallization. Heptane (1 mL) was added to a flask containing the reaction mixture then the flask was gently warmed with a heat gun causing the solid to dissolve. The resulting solution was left standing in the freezer. The resulting crystals were filtered to afford pure (*tropos*, *trans*)-**5** as a white solid (0.111 g, 0.166 mmol, 31 %). ^1H NMR (C_6D_6, 500 MHz) δ 7.21-7.02 (12H, m, ArH), 6.66 (2H, d, J = 2.9 Hz, ArH), 3.94-3.86 (1H, m, CH_2-O), 3.69-3.61 (1H, m, CH_2-O), 3.42-3.36 (1H, m, P-CH), 3.31 (3H, s, OCH_3), 3.30 (3H, s, OCH_3), 3.12-3.07 (1H, m, P-CH), 2.27-2.19 (1H, m, CH-CH_2), 2.00-1.88 (2H, m, CH-CH_2), 1.75-1.68 (1H, m, P-CH_2), 1.64-1.55 (1H, m, CH-CH_2), 1.47 (9H, s, 3 x CH3), 1.44 (9H, s, 3 x CH3), 1.41-1.35 (1H, m, P-CH_2). $^{31}P\{^1H\}$ NMR (C_6D_6, 202 MHz) δ 134.3 (s); 5.9 (s). ^{13}C NMR (C_6D_6, 126 MHz) δ 155.96 (ArC), 155.93 (ArC), 144.87 (ArC), 144.73 (ArC), 142.59 (ArC), 142.19 (ArC), 142.12 (ArC), 138.72 (ArC), 133.93 (ArC), 133.80 (ArC), 128.46-125-75 (m, 10 x ArCH), 114.60 (ArCH), 114.53 (ArCH), 112.94 (ArCH), 112.88 (ArCH), 63.03 (d, $^2J_{C\text{-}P}$ = 29.6 Hz, OCH_2), 54.74 (OCH3), 54.72 (OCH3), 50.66 (d, $^1J_{C\text{-}P}$ = 17.0 Hz, P-CH), 45.98 (d, $^1J_{C\text{-}P}$ = 15.6 Hz, P-CH), 37.61 (CH-CH_2), 35.18 ($C(CH_3)_3$), 35.15 ($C(CH_3)_3$), 31.83 (d, $^2J_{C\text{-}P}$ = 4.2 Hz, CH-CH_2), 30.59 (C(CH_3)$_3$), 30.59 (C(CH_3)$_3$), 28.22 (d, $^1J_{C\text{-}P}$ = 26.2 Hz, P-CH_2). HRMS (ES^+) $C_{40}H_{49}O_5P_2$ $[MH]^+$ m/z: 671.3041 found, 671.3050 required.

4,8-di-tert-butyl-6-(((R)-3-((2R,5R)-2,5-diphenylphospholan-1-yl)-1,1,1-trifluoropropan-2-yl)oxy)-2,10-dimethoxydibenzo[d,f][1,3,2]dioxaphosphepine and enantiomer, ***9a.*** 3,3'-di-*tert*-butyl-5,5'-dimethoxy-[1,1'-biphenyl]-2,2'-diol (0.342 g, 0.955 mmol) was placed in a Schlenk tube and dissolved in 3 mL of THF. The resulting solution was cooled to −78 ºC and PCl_3 (0.1 mL, 1.146 mmol) was added slowly. NEt_3 (0.4 mL, 2.865 mmol) was also added to the reaction mixture, which was then stirred and allowed to reach room temperature overnight, 16 h. The suspension was filtered using a frit under an inert atmosphere, and the filtrate was evaporated using a Schlenk line and dried under vacuum to remove any residual PCl_3. The crude $^{31}P\{^1H\}$ NMR (202.4 MHz, C_6D_6) spectrum showed a single peak at δ 172.0 ppm, corresponding to the chlorophosphite. The product was used in the next step without further purification. To a Schlenk flask containing a solution of the chlorophosphite from the previous step in toluene (4 mL) was added a solution of (*rac*,*trans*)-phospholane **6a** (major isomer) (0.311 g, 0.85 mmol) in toluene (5.5 mL) followed by a solution of 1,4-diazabicyclo-[2,2,2]-octane (DABCO) (0.476 g, 4.25 mmol, 5 eq.) in toluene (4.7 mL). The reaction mixture was then allowed to stir at room temperature overnight (19 h). The resulting suspension was filtered through silica gel (previously dried overnight in an oven) under an inert atmosphere, using dry toluene to compact and wash the SiO_2 after filtration. The resulting solution was evaporated under reduced pressure to afford the desired product as a white solid (0.44 g, 0.59 mmol, 69 %). ^1H NMR (C_6D_6, 500 MHz) δ 7.20-7.01 (12H, m, ArH), 6.64 (1H, d, J = 3.0 Hz, ArH), 6.62 (1H, d, J = 3.0 Hz, ArH), 4.55-4.45 (1H, m, CH-O), 3.45-3.35 (1H, m, P-CH), 3.31 (3H, s, OCH_3), 3.28 (3H, s, OCH_3), 3.06-3.10 (1H, m, P-CH), 2.26-2.18 (1H, m, P-CH-CH_2), 1.98-1.92 (1H, m, P-CH-CH_2), 1.89-1.80 (2H, m, P-CH-CH_2, P-CH_2), 1.63-1.53 (2H, m, P-CH-CH_2, P-CH_2), 1.45 (9H, s, 3 x CH3), 1.41 (9H, s, 3 x CH3). $^{31}P\{^1H\}$ NMR (C_6D_6), 202 MHz δ 143.9 (dq, $J_{P\text{-}P}$ = 32.6 Hz, $J_{P\text{-}F}$ = 7.0 Hz), 1.2 (br s). ^{19}F NMR (C_6D_6, 470 MHz) δ −76.30 (br s). ^{13}C NMR (C_6D_6, 126 MHz) δ 156.25 (ArC), 156.03 (ArC), 144.15 (d, $J_{C\text{-}P}$ = 17.5 Hz, ArC), 142.75 (ArC), 142.35 (ArC), 141.76 (d, $J_{C\text{-}P}$ = 7.9 Hz, ArC), 141.24 (ArC), 138.27 (ArC), 134.27 (ArC), 133.72 (ArC), 128.50-127-50 (m, 8 x ArCH), 126.18 (ArCH), 125.90 (ArCH), 124.41 (qm, $^1J_{C\text{-}F}$ = 283 Hz, CF_3), 114.55 (ArCH), 114.52 (ArCH), 113.07 (ArCH), 112.92 (ArCH), 71.42-70.62 (m, OCH), 54.72 (2 x OCH3), 51.23 (d, $^1J_{C\text{-}P}$ = 17.9 Hz, P-CH), 45.93 (d, $^1J_{C\text{-}P}$ = 16.1 Hz, P-CH), 37.56 (P-CH-CH_2), 35.24 ($C(CH_3)_3$), 35.17 ($C(CH_3)_3$), 31.89 (d, $^2J_{C\text{-}P}$ = 3.7 Hz, P-CH-CH_2), 31.04 (C(CH_3)$_3$), 30.66 (d, $J_{C\text{-}P}$ = 2.7 Hz, C(CH_3)$_3$), 27.10 (d, $^1J_{C\text{-}P}$ = 32.1 Hz, P-CH_2). HRMS (ES^+) $C_{41}H_{48}O_5F_3P_2$ $[MH]^+$ m/z: 739.2908 found, 739.2924 required.

4,8-di-tert-butyl-6-((S)-3-((2R,5R)-2,5-diphenylphospholan-1-yl)-1,1,1-trifluoropropan-2-yl)oxy)-2,10-dimethoxydibenzo[d,f][1,3,2]dioxaphosphepineand enantiomer, ***9b.*** The compound was prepared as described above for **9a** from 3,3'-di-*tert*-butyl-5,5'-dimethoxy-[1,1'-biphenyl]-2,2'-diol (0.342 g, 0.955 mmol), PCl_3 (0.1 mL, 1.146 mmol) and (*rac*,*trans*)-phospholane **6b** (minor isomer) (0.293 g, 0.80 mmol). White solid (0.44 g, 0.59 mmol, 41 %). Recrystallization from heptane afforded X-Ray quality crystals to determine the absolute configuration of the ligand (in racemic form). ^1H NMR (C_6D_6, 500 MHz) δ 7.21-7.03 (12H, m, ArH), 6.67 (1H, d, J = 2.9 Hz, ArH), 6.60 (1H, d, J = 3.0 Hz, ArH), 3.48-3.41 (1H, m, P-CH), 3.36-3.29 (1H, m, CH-O), 3.30 (3H, s, OCH_3), 3.27 (3H, s, OCH_3), 2.68-2.63 (1H, m, P-CH), 2.17-2.09 (1H, m, P-CH-CH_2), 1.93-1.83 (2H, m, P-CH-CH_2, P-CH_2), 1.77-1.69 (1H, m, P-CH-CH_2), 1.57-1.44 (2H, m, P-CH-CH_2, P-CH_2), 1.44 (9H, s, 3 x CH3), 1.27 (9H, s, 3 x CH3). $^{31}P\{^1H\}$ NMR (C_6D_6), 202 MHz δ 142.5 (d, $J_{P\text{-}P}$ = 41.5 Hz), −3.8 (br s). ^{19}F NMR (C_6D_6, 471 MHz) δ −77.62 (s). ^{13}C NMR (C_6D_6, 126 MHz) δ 156.44 (ArC), 155.61 (ArC), 144.01 (ArC), 143.86 (ArC), 142.91 (ArC), 142.60 (ArC), 140.67 (ArC), 137.36 (ArC), 135.00 (ArC), 132.85 (ArC), 128.84-127-50 (m, 8 x ArCH), 126.17 (ArCH), 126.09 (ArCH), 124.15 (qm, $^1J_{C\text{-}F}$ = 227 Hz, CF_3), 114.75 (ArCH), 114.45 (ArCH),

113.16 (ArCH), 112.40 (ArCH), 70.92-69.89 (m, OCH), 54.71 (2 x OCH3), 51.37 (d, $^{1}J_{C\text{-}P}$ = 16.7 Hz, P-CH), 46.02 (d, $^{1}J_{C\text{-}P}$ = 16.7 Hz, P-CH), 38.35 (P-CH-CH_2), 35.25 ($C(CH_3)_3$), 35.06 ($C(CH_3)_3$), 31.15 (d, $^{2}J_{C\text{-}P}$ = 3.6 Hz, P-CH-CH_2), 30.72 (d, $J_{C\text{-}P}$ = 3.9 Hz, $C(CH_3)_3$), 30.42 ($C(CH_3)_3$), 27.19 (d, $^{1}J_{C\text{-}P}$ = 30.2 Hz, P-CH_2). HRMS (ES^+) $C_{41}H_{48}O_5F_3P_2$ $[MH]^+$ m/z: 739.2912 found, 739.2924 required.

Computational Details. The same DFT protocol as in our previous study on BOBPHOS[7d] was used, except that the D3 dispersion corrections were already involved at the level of the optimisations. Specifically structures were optimised in the gas phase at the RI-BP86-D3/SDD(Rh)/6-31G** level, followed by evaluation of the harmonic vibrational frequencies at the same level (which were also used to calculate thermodynamic corrections to free energies) and refinement of the energies through single points at the B3PW91-D3/SDD(Rh)/6-31+G**/PCM_{MeOH} level (including a continuum solvation model. See ESI for further details and references.

ASSOCIATED CONTENT

Supporting Information

The Supporting Information is available free of charge on the ACS Publications website.

Experimental procedures ^{1}H, ^{31}P, ^{13}C NMR and HPIR spectra (PDF). X-ray data (PDF). Further computational details, tabular and graphical material, as well as optimised structures. Crude underpinning data is also available.[18]
CCDC 2059396 contains the supplementary crystallographic data for this paper. These data can be obtained free of charge via www.ccdc.cam.ac.uk/data_request/cif, or by emailing data_request@ccdc.cam.ac.uk, or by contacting The Cambridge Crystallographic Data Centre, 12 Union Road, Cambridge CB2 1EZ, UK; fax: +44 1223 336033.

AUTHOR INFORMATION

Corresponding Author

*Matthew L. Clarke – School of Chemistry, University of St. Andrews, St. Andrews KY16 9ST, U.K.; orcid.org/0000-0002-2444-1244; Email: mc28@st-andrews.ac.uk. For correspondence regarding DFT calculations, contact mb105@st-andrews.ac.uk.

Authors

José A. Fuentes, Michael Bühl, Alexandra M. Z. Slawin, Matthew L. Clarke – School of Chemistry, University of St. Andrews, St. Andrews KY16 9ST, U.K.
Mesfin E. Janka - Eastman Chemical Company, 200 South Wilcox Drive, Kingsport, Tennessee, 37660, USA.
Jody Rodgers - Eastman Chemical Company, 200 South Wilcox Drive, Kingsport, Tennessee, 37660, USA.
Kevin J. Fontenot - Eastman Chemical Company, 200 South Wilcox Drive, Kingsport, Tennessee, 37660, USA.

Notes

The authors declare no competing financial interest.

ACKNOWLEDGMENT

This paper is dedicated to the memory of a former colleague, Professor Paul Kamer (1960-2020): always so enthusiastic about making ligands and studying hydroformylation. We thank the Eastman Chemical Company for funding and permission to publish. M. B. thanks the School of Chemistry and EaStCHEM for support. Calculations were performed on a local HPC cluster maintained by Dr H. Früchtl. We thank Michelle Tittle for technical assistance with the stability testing carried out at Eastman Chemicals.

REFERENCES

(1) (a) van Leeuwen, P. W. N. M. in Rhodium Catalyzed Hydroformylation, Vol. 22 (Eds.: van Leeuwen, P. W. N. M.; Claver, C.), Springer Netherlands, Dordrecht, **2002**, pp. 1–13; (b) Franke, R. Selent, D.; Börner, A. Applied hydroformylation. Chem. *Rev.* **2012**, *112*, 5675–5732; (c) Börner, A.; Franke, R. in Hydroformylation. fundamentals, processes, and applications in organic synthesis, (Eds. Börner, A.; Franke, R.), Wiley-VCH, Weinheim, **2016**.

(2) (a) The global demand for iso-butanal was estimated to be over half a million tonnes in 2014. Grand view research, Mar **2016**, Isobutanol market analysis by product (synthetic, bio-based), application (oil & gas, solvents & coatings, chemical intermediates) and segment forecasts to 2022, https://www.grandviewresearch.com/industry-analysis/isobutanol-market.; (b) The branched isomer from hydroformylation of functionalized alkenes like styrene derivatives is readily formed and already has viable catalysts. See for example: Axtell, A. T.; Cobley, C. J.; Klosin, J.; Whiteker, G. T.; Zanotti-Gerosa, A.; Abboud, K. A. *Angew. Chem. Int. Ed*. **2004**, *44*, 5834; (c) (c) Watkins, A. V.; Hashiguchi, B. G.; Landis, C. R. *Org. Lett*. **2008**, *10*, 4553.

(3) (a) L. Gonsalvi, A. Guerriero, E. Monflier, F. Hapiot, M. Peruzzini in Hydroformylation for organic synthesis, Vol. 342 (Eds.: M. Taddei, A. Mann), Springer Berlin Heidelberg, Berlin, **2013**, pp. 1–47. (b) T. J. P. Devon, G. W. Puckette, T. A. Stavinoha, J. L. Vanderbilt (Eastman Kodak Company). Chelate ligands for low pressure hydroformylation catalyst and process employing same. US 4694109 A, **1987**; (c) T. J. P. Devon, G. W. Puckette, T. A. Stavinoha, J. L. Vanderbilt (Eastman Kodak Company). Hydroformylation process using novel phosphine-rhodium catalyst system. US 5332846 A, **1994**; (d) C. P. Casey, E. L. Paulsen, E. W. Beuttenmueller, B. R. Proft, L. M. Petrovich, B. A. Matter, D. R. Powell. Electron withdrawing substituents on equatorial and apical phosphines have opposite effects on the regioselectivity of rhodium catalyzed hydroformylation. *J. Am. Chem. Soc.* **1997**, *119*, 11817 –11825; (e) C. P. Casey, E. L. Paulsen, E. W. Beuttenmueller, B. R. Proft, B. A. Matter, D. R. Powell. Electronically dissymmetric DIPHOS derivatives give higher n:i regioselectivity in rhodium-catalyzed hydroformylation than either of their symmetric counterparts. *J. Am. Chem. Soc.* **1999**, *121*, 63–70. (f) E. Billig, A. G. Abatjoglou, D. R. Bryant (Union Carbide). Bis(phosphite) complexes as hydroformylation catalyst precursors. EP 213639, **1987**. (g) L. A. van der Veen, M. D. K. Boele, F. R. Bregman, P. C. J. Kamer, P. W. N. M. van Leeuwen, K. Goubitz, J. Fraanje, H. Schenk, C. Bo. Electronic effect on rhodium diphosphine catalyzed hydroformylation: the bite angle effect reconsidered. *J. Am. Chem. Soc.* **1998**, *120*, 11616–11626, and references therein.

(4) (a) R. C. How, M. L. Clarke, R. T. Hembre, J. A. Ponasik, G. S. Tolleson (Eastman Chemical Company). Phosphorous compounds useful as ligands and compositions and methods regarding them. US 9308527 B2, **2016**; (b) R. C. How, R. Hembre, J. A. Ponasik, G. S. Tolleson, M. L. Clarke. A modular family of phosphine-phosphoramidite ligands and their hydroformylation catalysts: steric tuning impacts upon the coordination geometry of trigonal bipyramidal complexes of type $[Rh(H)(CO)_2(P\text{^}P^*)]$. *Catal. Sci. Technol.* ***2016***, *6*, 118–124; (c) R. C. How, P. Dingwall, R. T. Hem-

bre, J. A. Ponasik, G. S. Tolleson, M. L. Clarke. Composition of catalyst resting states of hydroformylation catalysts derived from bulky mono-phosphorus ligands, rhodium dicarbonyl acetylacetonate and syngas. *Mol. Catal.* **2017**, *434*, 116–122; (d) D. W. Norman, J. N. H. Reek, T. R. M.-L. Besset (Eastman Chemical Company). Catalysts and process for producing aldehydes. US 8710275 B2, **2014**; (e) n/iso of 0.84 at 25°C, 1.1 at 70°C: X. Wang, S. Nurttila, W. I. Czik, R. Becker, J. Rodgers, J. N. H. Reek. Tuning the porphyrin building block in self-assembled cages for branched-selective hydroformylation of propene. *Chem. Eur. J.* **2017**, *23*, 14769 –14777; (f) In contrast to BOBPHOS, Ph-bis-phospholano-ethane ligands gives a mixture of linear and branched isomers unless there is some modest electronic bias, see Yu, Z.; Eno, M. S.; Annis, A. H.; Morken, J. P. *Org. Lett*. **2015**, *17*, 3264.

(5) Iu, L.; Fuentes, J. A.; Janka, M. E.; Fontenot, K. J.; Clarke, M. L. High *iso* aldehyde selectivity in the hydroformylation of short-chain alkenes. *Angew. Chem. Int. Ed.* **2019**, *58*, 2120 –2124.

(6) (a) Zhang, B.; Jiao, H.; Michalik, D.; Kloß, S.; Deter, L. M.; Selent, D.; Spannenberg, A., Franke, R.; Börner, A. Hydrolysis stability of bidentate phosphites utilized as modifying ligands in the Rh-catalyzed *n*-regioselective hydroformylation of olefins. *ACS Catal.* **2016**, *6*, 7554-7565. (b) Börner, A.; Franke, R. Chapter 3 in Hydroformylation. Fundamentals, Processes, and Applications in Organic Synthesis; (Eds. Börner, A.; Franke, R.), Wiley-VCH:Weinheim, Germany, **2016**. (c) van Leeuwen, P.W.N.M.; Chadwick, J.C. chapter 3 and 5 in Homogeneous Catalysts. Activity—Stability—Deactivation;Wiley-VCH:Weinheim, Germany, **2011**. (d) Kloß, S. Selent, D.; Spannenberg, A.; Franke, R.; Börner, A.; Sharif, M. Effects of substitution pattern in phosphite ligands used in rhodium-catalyzed hydroformylation on reactivity and hydrolysis stability. *Catalysts*, **2019**, *9*, 1036.

(7) (a) G. M. Noonan, J. A. Fuentes, C. J. Cobley, M. L. Clarke. An Asymmetric Hydroformylation Catalyst that Delivers Branched Aldehydes from Alkyl Alkenes. *Angew. Chem. Int. Ed.* **2012**, *51*, 2477–2480; *Angew. Chem.* **2012**, *124*, 2527–2530; (b) G. M. Noonan, C. J. Cobley, T. Mahoney, M. L. Clarke. Rhodium/phospholane–phosphite catalysts give unusually high regioselectivity in the enantioselective hydroformylation of vinyl arenes. *Chem. Commun.* **2014**, *50*, 1475–1477; (c) R. Pittaway, J. A. Fuentes, M. L. Clarke. Diastereoselective and branched-aldehyde-selective tandem hydroformylation–hemiaminal formation: synthesis of functionalized piperidines and amino alcohols. *Org. Lett.* **2017**, *19*, 2845–2848; (d) P. Dingwall, J. A. Fuentes, L. Crawford, A. M. Z. Slawin, M. Bühl, M. L. Clarke. Understanding a Hydroformylation catalyst that produces branched aldehydes from alkyl alkenes. *J. Am. Chem. Soc.* **2017**, *139*, 15921–15932; (e) (S_{ax},*S*,*S*)-BOBPHOS is commercially available from Strem Chemicals.

(8) (a) Czauderna, C. F.; Cordes, D. B.; Slawin, A. M. Z.; Müller, C.; van der Vlugt, J. I.; Vogt, D.; Kamer, P. C. J. Synthesis and reactivity of chiral, wide-Bite-angle, hybrid diphosphorus ligands. *Eur. J. Inorg. Chem.* **2014**, *2014*, 1797–1810. (b) del Río, I.; Pa mies, O.; van Leeuwen, P. W. N. M.; Claver, C. Mechanistic study of the hydroformylation of styrene catalyzed by the rhodium/BDPP system. *J. Organomet. Chem.* **2000**, *608,* 115–121. (c) van der Veen, L. A.; Boele, M. D. K.; Bregman, F. R.; Kamer, P. C. J.; van Leeuwen, P. W. N. M.; Goubitz, K.; Fraanje, J.; Schenk, H.; Bo, C. Electronic effect on rhodium diphosphine catalyzed hydroformylation: the bite angle effect reconsidered. *J. Am. Chem. Soc.* **1998**, *120*, 11616–11626. (d) Chikkali, S. H.; van der Vlugt, J. I.; Reek, J. N. H. Hybrid diphosphorus ligands in rhodium catalysed asymmetric hydroformylation. *Coord. Chem. Rev.* **2014**, *262*, 1–15.

(9) (a) C. P. Casey, G. T. Whiteker, M. G. Melville, L. M. Petrovich, J. A. Gavney, D. R. Powell. Diphosphines with natural bite angles near 120.degree. increase selectivity for n-aldehyde formation in rhodium-catalyzed hydroformylation. *J. Am. Chem. Soc.* **1992**, *114*, 5535-5543. (b) G. J. H. Buisman, L. A. van der Veen, P. C. J. Kamer, P. W. N. M. van Leeuwen. Fluxional Processes in Asymmetric Hydroformylation Catalysts [HRhL⌒L(CO)$_2$] Containing C_2-Symmetric Diphosphite Ligands. Organometallics, **1997**, *16*, 5681-5687. (c) L. L. J. M. Cornelissen PhD thesis. Metal-catalyzed asymmetric hydroformylation: towards the understanding of stereoselection processes. Technical University of Eindhoven, (Prof D. Vogt research group), available from: https://pure.tue.nl/ws/files/3216842/ 200911591.pdf.

(10) For NMR studies of phosphine-phosphites see: (a) Deerenberg, S.; Kamer, P. C. J.; van Leeuwen, P. W. N. M. New chiral phosphine–phosphite ligands in the enantioselective rhodium-catalyzed hydroformylation of styrene. *Organometallics* **2000**, *19*, 2065–2072. (b) Pàmies, O.; Net, G.; Ruiz, A.; Claver, C. Asymmetric hydroformylation of styrene catalyzed by furanoside phosphine–phosphite–Rh(I) complexes. *Tetrahedron: Asymmetry* **2001**, *12*, 3441–3445. (c) Rubio, M.; Suárez, A.; Alvarez, E.; Bianchini,C.; Oberhauser, W.; Peruzzini, M.; Pizzano, A. Asymmetric hydroformylation of olefins with Rh catalysts modified with chiral phosphine–phosphite ligands. *Organometallics* **2007**, *26*, 6428–6436. (d) Robert, T.; Abiri, Z.; Wassenaar, J.; Sandee, A.J.; Romanski, S.; Neudörfl, J.-M.; Schmalz, H.-G.; Reek, J. N. H. Asymmetric hydroformylation using Taddol-based chiral phosphine–phosphite ligands. *Organometallics* **2010**, *29*, 478–483. (e) Nozaki, K.; Sakai, N.; Nanno, T.; Higashijima, T.; Mano, S.; Horiuchi, T.; Takaya, H. Highly enantioselective hydroformylation of olefins catalyzed by rhodium(I) complexes of new chiral phosphine–phosphite ligands. *J. Am. Chem. Soc.* **1997**, *119*, 4413–4423. (f) Castillo-Molina, D. A.; Casey, C. P.; Müller, I.; Nozaki, K.; Jäkel, C. New low-temperature NMR studies establish the presence of a second equatorial–apical isomer of [(*R*,*S*)-Binaphos](CO)$_2$RhH. *Organometallics* **2010**, *29*, 3362-3367.

(11) (a) Christiansen, A.; Selent, D.; Spannenberg, A.; Köckerling, M.; Reinke, H.; Baumann,W.; Jiao, H.; Franke, R.; Börner. Heteroatom-substituted secondary phosphine oxides (HASPOs) as decomposition products and preligands in rhodium-catalysed hydroformylation. *Chem. Eur. J.* **2011**, *17*, 2120–2129; (b) Morales Torres, G.; Behrens, S. Michalik, D.; Selent, D.; Spannenberg, A.; Luhr, S.; Dyballa, K. M.; Franke, R.; Börner, A, Synthesis of C2-symmetric diphosphoramideite and their use as ligands in Rh-catalyzed hydroformylation: relationships between activity and hydrolysis stability, *Chem. Open*, **2017**, *6*, 247.

(12) (a) Allman, T.; Goel, R. G. The basicity of phosphines. *Can. J. Chem.* **1982**, *60*, 716–722. (b) Howell, J. A. S.; Lovatt, J. D.; McArdle, P.; Cunningham, D. Maimone, E.; Gottlieb, H. E.; Goldschmidt, Z. The effect of fluorine, trifluoromethyl and related substitution on the donor properties of triarylphosphines towards [Fe(CO)$_4$]. *Inorg. Chem. Commun.* **1998**, *1*, 118–120. (c) Sowa, J. R.; Agelici, R. J. Bidentate phosphine basicities as determined by enthalpies of protonation. *Inorg. Chem.* **1991**, *30*, 3534–3537. (d) Rahman, M. M.; Liu, H.-Y.; Eriks, K.; Prock, A.; Giering, W. P. Quantitative analysis of ligand effects. Part 3. Separation of phosphorus(III) ligands into pure .sigma.-donors and .sigma.-donor/.pi.-acceptors. Comparison of basicity and .sigma.-donicity. *Organometallics* **1989**, *8*, 1–7.

(13) (a) For the synthesis of the chlorophosphite from the *tropos* diol see ref 11 and references therein. (b) for the identity of the byproduct see: Selent, D.; Hess, D.; Wiese, K.D.; Rotger, D.; Kunze, C.; Borner, A. New phosphorus ligands for the rhodium-catalyzed isomerization/hydroformylation of internal octenes. *Angew. Chem. Int. Ed.* **2001**, *40*, 1696 –1698.

(14) Jiao, Y.; Serrano Torne, M.; Gracia, J.; Niemantsverdriet, J. W (H.).; van Leeuwen, P. W. N. M. Ligand effects in rhodium-catalyzed hydroformylation with bisphosphines: steric or electronic? *Catal. Sci. Technol.* **2017**, *7*, 1404–1414.

(15) DeJongh, D. C.; Van Fossen, R. Y. Mass spectra and pyrolyses of *o*-phenylene sulfite and related compounds. *J. Org. Chem.* **1972**, *37*, 1129–1135.

(16) Jonas, V.; Thiel, W. Theoretical study of the vibrational spectra of the transition metal carbonyls M(CO)6 [M=Cr, Mo, W], M(CO)5 [M=Fe, Ru, Os], and M(CO)4[M=Ni, Pd, Pt]. J. Chem. Phys. 1995, 102, 8474–8484.

(17) Hood, D. M.; Johnson, R. A.; Carpenter, A. E. ; Younker, J. M.; Vineyard, D. J.; Stanley, G. G. Highly active cationic cobalt(II) hydroformylation catalysts, *Science*, **2020**, *367*, 542.

(18) Fuentes García, J. A., Janka, M. E., Rodgers, J., Fontenot, K. J., Buehl, M., Slawin, A. M. Z., Clarke, M., 2021, Effect of Ligand Backbone on the Selectivity and Stability of Rhodium Hydroformylation Catalysts Derived from Phospholane-Phosphites (dataset). Dataset. University of St Andrews Research Portal. https://doi.org/10.17630/285dd924-a77e-4578-9455-ea41c85cc3f1